Neurochirurgie 57 (2011) 52–67

Disponible en ligne sur ScienceDirect www.sciencedirect.com

Elsevier Masson France EM|consulte www.em-consulte.com

Original article

White matter anatomy of the human deep brain revisited with high resolution DTI fibre tracking

Anatomie de la substance blanche du cerveau profond revisitée en tractographie à partir d'imagerie haute résolution par tenseur de diffusion

J.-J. Lemaire[a,*,b], G. Cosnard[c], L. Sakka[a,b], C. Nuti[b,d], W. Gradkowski[c,e], S. Mori[f,g], L. Hermoye[c,e]

[a] *Service de neurochirurgie A, hôpital Gabriel-Montpied, CHU de Clermont-Ferrand, BP 69, 63003 Clermont-Ferrand cedex 1, France*
[b] *EA 3295, équipe de recherche en signal et imagerie médicale, Clermont université, université d'Auvergne, BP 10448, 63000 Clermont-Ferrand, France*
[c] *Diagnostic Radiology Unit, Saint-Luc University Hospital, université Catholique de Louvain, Brussels, Belgium*
[d] *Service de neurochirurgie, hôpital Bellevue, CHU de Saint-Étienne, 42055 Saint-Étienne, France*
[e] *Imagilys SPRL, Brussels, Belgium*
[f] *Department of Radiology and Radiological Science, Johns Hopkins University School of Medicine, Baltimore, Maryland*
[g] *F. M. Kirby Research Centre for Functional Brain Imaging, Kennedy Krieger Institute, Baltimore, Maryland*

ARTICLE INFO

Article history:
Received 7 September 2010
Accepted 21 March 2011
Available online 30 April 2011

Keywords:
Connectivity
Deep brain
Diffusion tensor imaging
Fascicles
Fibre tracking
White matter

ABSTRACT

Background and Purpose. – Deep white matter (WM) fascicles play a major, yet poorly understood, role in the overall connectivity of human brain. Better knowledge of their anatomy is requisite to understand the clinical correlates of their lesions and develop targeted treatments. We investigated whether MR-based diffusion tensor imaging (DTI) and fibre tracking could reveal in vivo, in explicit details, the 3D WM architecture within the subthalamic region and the internal capsule.
Methods. – High-resolution DTI images were acquired on six healthy volunteers on a three Tesla MR scanner. We studied using single-subject analysis WM fascicles within the subthalamic region and the internal capsule, as follows: DTI deterministic fibre tracking (FT) of fascicles; embedding fascicles in the volume-rendered brain coupled with a triplanar view; rigorous anatomic labelling of each fascicle according to classical knowledge as described by pioneer neuroanatomists. Deterministic FT effects were taken into account.
Results. – We charted most of WM fascicles of the deep brain, in particular large and complex fascicles such as the basal forebrain bundle and the ansa lenticularis. A topographic classification of subthalamic fascicles was proposed into three groups: the cerebellorubral, the reticulo-dorsal and the tegmento-peripheral one.
Conclusions. – Beyond to demonstrate the feasibility of imaging the deepest WM fascicles in vivo, our results pave the way for a better understanding of the brain connectivity and for developing targeted neuromodulation.

Mots clés :
Connectivité
Cerveau profond
Imagerie par tenseur de diffusion
Faisceaux
Tractographie
Substance blanche

RÉSUMÉ

Objectif. – Les faisceaux profonds de la substance blanche (SB) jouent un rôle majeur, encore incomplètement étudié, dans la connectivité globale du cerveau. Une meilleure connaissance de leur anatomie est nécessaire pour comprendre l'impact de lésions et pour développer de nouveaux traitements ciblés. Nous avons cherché à évaluer l'imagerie par résonance magnétique (IRM) nucléaire en tenseur de diffusion (ITD) et la tractographie, pour explorer de manière détaillée l'architecture tridimensionnelle de la SB dans la région sous thalamique et la capsule interne.
Méthode. – Des images ITD en haute résolution ont été acquises chez six volontaires sur une machine IRM à trois teslas. Les faisceaux de SB ont été étudies selon une approche par individu : tractographie

* Corresponding author.
E-mail address: jjlemaire@chu-clermontferrand.fr (J.-J. Lemaire).

0028-3770
doi:10.1016/j.neuchi.2011.04.001

déterministe des faisceaux à partir de l'ITD ; incorporation des faisceaux dans le cerveau reconstruit à partir de l'IRM et analyse 3D triplanaire ; labellisation anatomique rigoureuse de chaque faisceau à partir des connaissances anatomiques classiques. Les effets confondants en tractographie déterministique ont été intégrés.

Résultat. – Nous avons cartographié la plupart des faisceaux du cerveau profond, en particulier ceux larges et complexes comme le faisceau basal du cerveau antérieur et l'anse lenticulaire. Une classification topographique en trois groupes des faisceaux sous-thalamiques est proposée : cérébello-rubral, réticulo-dorsal et tegmento-périphérique.

Conclusion. – Au-delà de la faisabilité d'explorer les faisceaux les plus profonds de la SB, in vivo, nos résultats permettent d'envisager une meilleure compréhension de la connectivité cérébrale et le développent de neuromodulation ciblée.

1. Introduction

In the last decade, increased understanding of the role of deep brain processes and connectivity in neurological and psychiatric disorders (Filley, 2001), as well as the success of deep brain stimulation in alleviating symptoms of several of these disorders – movement disorders (Benabid et al., 1996), epilepsy (Andrade et al., 2006), obsessive-compulsive disorder (Greenberg et al., 2006) and disorders of consciousness (Schiff et al., 2007) – have fostered new research to better understand both the structural and functional anatomy of the deep brain. The knowledge of the macroscopic structural anatomy that concerns nuclei and their connectivity is pre-required to analyse or modulate functions in neurosurgical applications. Whereas major deep nuclei have been largely explored, little progress has been made in the understanding of connectivity supported by WM fascicles. Fascicles of the human brain were described by pioneering anatomists at the end of the nineteenth and beginning of the twentieth century (Dejerine, 1901; Forel, 1877; Riley, 1953; Talairach et al., 1957). The human brain was extensively explored using post-mortem dissections and histological analysis of pathologic and healthy brain samples. WM fascicles were also studied using anatomic dissections after brain hardening techniques (see: Dejerine, 1901, for a review). Broadly it was the era of the "anatomo-clinical approach" that analysed relationships between clinical symptoms and brain anatomy (Goetz, 2000). Thanks to the progress of medical imaging techniques, the detailed organization of the human brain is now accessible in vivo, and used reliably in neurosurgery, like for the implantation of deep brain stimulation electrodes (Lemaire et al., 2007). However, in clinical practice, the 3D organization of the fascicles of the deep brain is still difficult to master.

It is only recently that diffusion tensor imaging (DTI) coupled with fibre tracking has made it possible to reveal individual tracks in vivo. Although the exact nature of the WM fascicles is still unknown, it comprises axons organized in bundles of fibres, arranged roughly in parallel with each other, creating a homogenous anatomic structure visible macroscopically or with low magnification (Hirano and Llena, 1995). DTI, which is sensitive to the anisotropic diffusion of protons in the fascicles, can generate maps of the WM fibres (Basser et al., 1994; Mori and Zhang, 2006), yielding atlas representations of main fascicles (Mori et al., 2005; Hermoye et al., 2006).

Deep white matter (WM) fascicles play a major, yet poorly understood, role in the overall connectivity of human brain. Better knowledge of their anatomy is requisite to understand the clinical correlates of their lesions and develop targeted treatments. In this study, we have used high resolution DTI and deterministic fibre tracking to reveal, in explicit details, the 3D WM architecture within the subthalamic region and the limbs of the internal capsule. We give a meticulous description of the anatomical course of each of the fascicles taking into account confounding deterministic FT effects. A glossary is provided (Supplementary Material 1: glossary).

2. Materials and methods

2.1. Subjects

Six healthy volunteers (three males, three females; mean age = 31 years, range, 25–50 years) were included after Institutional Review Board approval and written informed consent provided.

2.2. MRI data acquisition

Images were acquired using a sensitivity encoding head coil on a 3-Tesla whole-body MR scanner (Achieva, Philips Medical Systems, Best, Netherlands) equipped with explorer gradients (80 mTesla/m) and an 8-element arrayed RF coil. For DTI, a single-shot spin-echo echo-planar sequence was used with diffusion gradients in 32 non-collinear directions ($b = 1000 s/mm^2$). One reference image with the least diffusion weighting ($b = 33 s/mm^2$) was also acquired. Twenty-four axial slices were acquired along the cranial base from the pons to the caudate nucleus. Imaging parameters were as follows: field of view = 240 mm, acquisition matrix (rectangular field of view) = 192×113 pixels, bandwidth = 1117 Hz/pixel, slice thickness = 1.5 mm, voxel size $1.25 \times 1.25 \times 1.5\,mm^3$; all images were zero-filled to a final reconstruction matrix of 256×256 (reconstructed voxel size: $0.94 \times 0.94 \times 1.5\,mm^3$); repetition time = 3800 ms; echo time = 93 ms; SENSE reduction factor = 2.5, acquisition time = 4 min, 18 sec. To improve the signal-to-noise ratio, five identical datasets were acquired and averaged, leading to a total acquisition time of 21 min, 30 sec. A dual echo T2-weighted sequence (voxel size = $0.94 \times 0.94 \times 1.5\,mm^3$) was acquired for anatomical guidance (particularly the identification of deep nuclei). The head was held in place by a vacuum-molded cushion to minimize movement artifacts.

2.3. Diffusion tensor imaging fibre tracking

DTI analysis and fibre tracking were processed with DTI Studio (Jiang et al., 2006). Maps of the white matter tracts were computed by coding the main direction of diffusion of the protons in each voxel with the following convention: blue for inferior-superior (or vice versa), red for right-left, and green for anterior-posterior, with brightness proportional to the fractional anisotropy (Jiang et al., 2006). Quantitative maps of the fractional anisotropy (FA maps) were also computed in grayscale: from black (FA = 0) for totally isotropic-diffusion to white (FA = 1) for totally anisotropic diffusion.

Fibre tracking used a continuous tracking method (Mori and van Zijl, 2002; Mori et al., 1999), with a FA threshold of 0.25 and a turning-angle below 70°. Tracking was performed from all pixels inside the brain (brute force approach). To individualize each bundle, regions of interest (ROIs) were manually positioned according to careful anatomical analysis (see below). Fibres that penetrated each region-of-interest (ROI) were assigned to a specific fibre bundle associated with the ROI. Because most fascicles have a complex

Table 1
Main hemispheric white matter bundles around the basal ganglia and thalamus, according to Dejerine (1901) and Riley (1953).
Principaux faisceaux hémisphériques de substance blanche autour des ganglions de la base et du thalamus, d'après Dejerine (1901) et Riley (1953).

Anatomic organization	Longitudinal fascicles		Long arced fascicle	Short arced associative fibres	Corpus callosum		Commissures		Trigone	Thalamic radiations (cortico-thalamic fibers)	
	Inferior	Superior			Part	Fibre					
Terminology	Temporo-occipital fascicle or fasciculus longitudinalis inferior	Arcuate fascicle (of Burdach), or frontal superior fascicle, or fasciculus longitudinalis superior		Arced fibres of Arnold or U-shaped fibers of Meynert (intergyral fibers)	Knee (terminated by the rostrum or beak)	Anterior forceps or minor forceps (of Arnold)	Anterior commissure (AC) or Commissura anterior or rostralis		Fornix or tractus cortico-mammillaris	Four fascicles or peduncles	Anterior (frontal)
		Superior fronto-occipital, or occip-itofrontal fascicle of Forel	Uncinate fascicle or fasciculus uncinatus		Body	Superior or dorsal plane	Posterior commissure (PC) or Commissura posterior or caudalis or dorsalis				Superior (parieto-fronto-rolandic)
		Fronto-occipital superior medial, or superior longitudinal fascicle, or			Splenium or roll	Superior or dorsal plane	Dorsal supraoptic commissure or Commissura supraoptica dorsalis	Pars dorsalis; commissure of Ganser or commissure anterior of the hypothalamus			Posterior (occipitopari-etal; optic radiation)
	Inferior fronto-occipital fascicle	fronto-occipital superior, or occipito-frontal superior, or, stratum reticulatum of the corona radiata, or subcallosal bundle			Tapetum	Belongs to the occipitofrontal fascicle of Forel (Dejerine (Dejerine 1895, 1901)) or corpus callosum fibers (commonly accepted)		Pars ventralis; commissure of Meynert			
							Commissure of Gudden or Commissura supraoptica ventralis				Inferior (occipi-totemporal): pulvinar contingent and inferior-intern peduncle
							Commissure of Forel or Commissura supramamillaris				

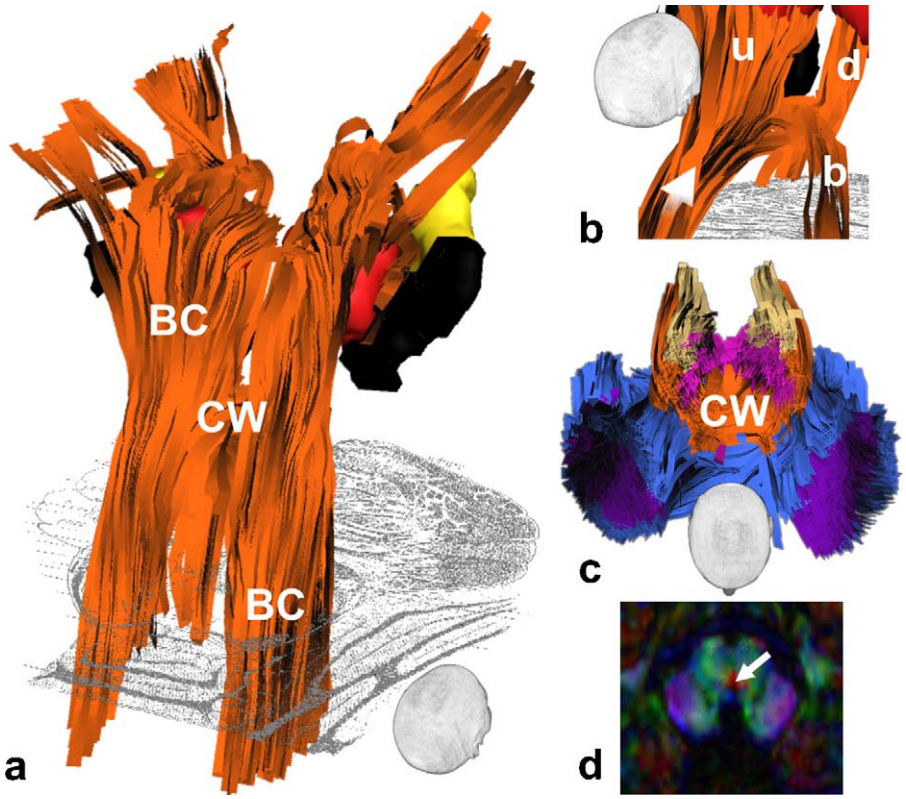

Fig. 1. The cerebellorubral group of subthalamic fibres (orange; subject no. 4): a: brachium conjonctivum (BC) and commissure of Wernekink (CW); b: uncrossed (u), bridging crossed (b) and decussating crossed (d) fibres of CW (the white arrow shows the origin of fibre tracking); c: section through the 3D block of mesencephalo-pontine fibres (pontine fibres, blue and purple; the reticulo-dorsal group of fibres, pink and beige); d: CW (white arrow) in an axial colour-coded map.
Groupe cérébello-rubral des fibres sous-thalamiques (orange; sujet no. 4) : a : brachium conjonctivum (BC) et commissure de Wernekink (CW) ; b : fibres, non croisées (u), croisées et en pont (b) et croisées et décussant (d) de CW (la flèche blanche indique l'origine de la tractographie) ; c : section dans le bloc 3D des fibres mésencéphalo-pontines (fibres pontines, bleu et violet; groupe de fibres réticulo-dorsales, rose et beige) ; d : CW (flèche blanche) sur une carte de direction codée par couleur dans un plan axial.

shape, several ROIs (from 2 to 6) were used to generate each fascicle composed of several fibre bundles. This anatomo-clinical approach was preferred to manually shaping bundles with logical operators (AND/NOT) after rough placement of ROIs. Each completed fibre bundle was exported into graphical software (Avizo 5.0.0, Mercury Computer Systems, MA, USA) for anatomical analysis on a volume-rendered brain coupled with an orthogonal viewer.

2.4. Anatomical analysis

The anatomic labelling of fascicles was realized in two steps: topographic analysis and comparison with classic anatomic knowledge (Supplementary Material 1: glossary). The topographic analysis consisted in the exploration of both the extremities and paths of fascicles, locally in each region, e.g. subthalamus, and globally (although limited by the stack of 24 axial slices going from the pons to the caudate nucleus). For anatomical guidance, structures were manually outlined on T2-weighted sequences or FA maps (Supplementary Material 2, which describes the anatomical landmarks); atlases (Morel et al., 1997; Olszewski and Baxter, 1954; Peel, 1954; Riley, 1953; Schaltenbrand and Bailey, 1959) were manually co-registered to the volume-rendered brain when necessary (Supplementary Material 3: glossary, which describes the atlas co-registrations). Image data sets (DTI, FA maps, and T2-weigthed images) were manually co-registered (linear affine registration; translation, rotation and scaling) minimizing the geometrical mismatch caused by DTI distortion and carefully controlled by visual analysis of several anatomic landmarks (nuclei, ventricles, corpus callosum and the envelope of the mesencephalon).

The final labelling was performed by comparing bundles of fibres displayed on 3D rendering with 2D anatomic diagrams, drawings and classic anatomic knowledge (Supplementary Material 1: glossary). To facilitate the anatomic analysis, fibres were displayed as colored ribbons using the same colour for fibres that belong to the same fascicle (e.g. Figs. 1–3). For each subject, the final anatomic labelling was accepted after complete 3D analysis of all the fascicles within the two studied regions, i.e. the subthalamus and the internal capsule (anterior and posterior limbs; sublenticular and retrolenticular segments). Because of the intricateness of deep brain fascicles we also explored fascicles related to the diencephalic-mesencephalic junction, whether they are anatomic neighbouring fibres or fibres embedded in the junction.

Practically, the individual subject analysis approach followed a learning curve to understand the 3D anatomy of WM fascicles (topography and organization) in one subject, then we identified and checked the WM bundles in the five others subjects. The classical, anatomy or knowledge (Supplementary Material 1: glossary) used as a reference in this study is summarized in Tables 1–3. The workflow of the entire study is shown in Supplementary Material (Supplementary Material 4, which shows an overview of the workflow). The broad qualitative analysis of the inter-subject variability of deep brain fascicles is provided.

3. Results

The subthalamic fibres were split into three topographic groups – the cerebellorubral, reticulo-dorsal, and tegmento-peripheral. This new organization was proposed after meticulous

Table 2
Main white matter bundles of the internal capsule, according to Dejerine (1901) and Riley (1953).
Principaux faisceaux de substance blanche de la capsule interne, d'après Dejerine (1901) et Riley (1953).

Anatomic organization	Anterior arm; lenticulo-caudate segment	Knee or genu	Posterior arm; lenticulo-optic segment				Retrolenticular segment	Sublenticular segment
			Superior tracts	Peduncular tracts	Lenticulate radiate fibres	Other		
Terminology	Fronto-thalamic projections		Corticodiencephalic	Corticomesencephalic	Lenticulo-thalamic radiations (dorsal location)	Fascicle of Türck (or Türck-Meynert) or tractus temporopontinus or fascicle temporo-occipito-protuberantial (of Flechsig)	Optic radiations (of Gratiolet) or radiatio optica; visual cortical fascicle (including the Meyer's loop)	Fascicle of Türck
	Lenticulo-caudate fibers	Geniculate fascicle		Corticopontine (including the fronto-pontine fascicle)	Strio-luysien radiations			
			Corticothalamic	Pyramidal tract	Ansa lenticularis			Fascicle of Arnold or temporo-thalamic fascicle of Arnold
	Fronto-pontine fascicle (tractus) of Arnold				Lenticular fascicle (of Forel)			

Table 3
Other brain fascicles, according to Dejerine (1901) and Riley (1953).
Autres faisceaux, d'après Dejerine (1901) et Riley (1953).

Anatomic organization	Lenticular radiate fibres		Forel's fields	Forebrain fascicles	Peduncular fascicle		Others		
	Strio-thalamic radiations	Strio-subthalamic radiations	Tegmental area				Longitudinal fascicles of the diencephalo-mesencephalic region		Superior cerebellar fascicles
Terminology	Contains the Ansa peduncularis	Lenticular fascicle (H2)	H1 fascicle (dorsal) or thalamic fascicle	Fronto-mesencephalic bundle	Fascicle of Türck		Medial longitudinal fascicle or fasciculus longitudinalis medialis		
		Strio-luysien fascicle			Corticopontine tract or tractus corticopontinus				
		Ansa lenticularis or Ansa of the lentiformis nucleus	H2 fascicle (ventral) or lenticular fascicle	Basal (or medial) forebrain bundle or medial telencephalic fascicle or fasciculus telencephalicus medialis	Pyramidal tract or tractus pyramidalis		Central tegmental tract or tractus tegmentalis centralis		Brachium conjunctivum with its decussation (tegmentum, dorsal and ventral parts) or Wernekink ("horseshoe") decussation
			Forel's H field (pre-rubral)		Aberrant fibers (medial); The more medial fibers appear predominantly crossed.	E.g. : (1) Stratum intermedium; (2) Oblique fascicle, fascicle "en écharpe" of Féré (fascicle circumligatus or obliquus)	Lemniscus	Medial or Lemniscus sensibilis or Reil median Lateral or Lemniscus acusticus	

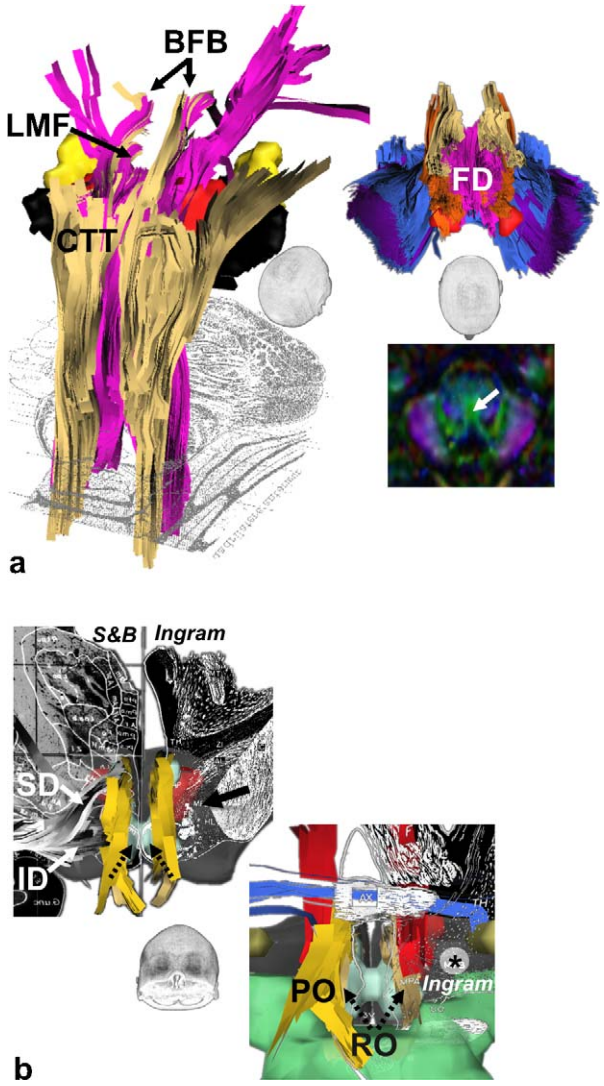

Fig. 2. The reticulo-dorsal group of subthalamic fibres: a: (subject no. 4) left: basal forebrain bundle (BFB), central tegmental tract (CTT), longitudinal medial fascicle (LMF) and the ventral tegmental decussation of Forel (FD); Top right, FD, section through the 3D block of mesencephalo-pontine fibres; bottom right, axial colour-coded map showing FD (white arrow); b: (subject no. 1) front views of BFB (gold): left, BFB (anteriorly to the mamillary bodies; black dotted arrows; registration: Schaltenbrand and Bailey's atlas (Schaltenbrand and Bailey, 1959), semi-schematic drawing from Ingram (Peel, 1954)) and the superior, SD, and inferior, ID, divisions of ansa lenticularis, are depicted (white arrows); right, BFB with the pre- (PO) and retro- optic (RO, black arrows) contingents, the representation according to Ingram (Peel, 1954) at the optic area is also depicted (*).
Groupe réticulo-dorsal des fibres sous-thalamiques : a : (sujet no. 4) à gauche : faisceau basal du cerveau antérieur (BFB), tractus tegmental central (CTT), faisceau longitudinal médial (LMF) et décussation tegmentale ventrale de Forel (FD) ; en haut à droite, FD, section dans le bloc 3D des fibres mésencéphalo-pontines ; en bas à droite, carte de direction codée par couleur dans un plan axial montrant FD (flèche blanche) ; b : (sujet no. 1) vues de face du BFB (doré) : à gauche, BFB (en avant des corps mamillaires ; flèches pointillées noires ; correspondance avec l'atlas de Schaltenbrand et Bailey (1959), dessin semi-schématique d'après Ingram (Peel, 1954)), et les divisions supérieure, SD, and inférieure, ID, de l'anse lenticulaire (flèches blanches) ; à droite, BFB avec les contingents pré- (PO) and rétro- optiques (RO, flèches noires), ainsi que la représentation d'après Ingram (Peel, 1954) dans la région optique (*).

analysis of the overall WM architecture showing the three well-organized groups, systematically identifiable. The internal capsule contained projection tracts (Supplementary Material 1: glossary) to deep nuclei and the brainstem (the lower brainstem and spinal cord fibres could not be followed), and the largest, non-commissural, connective bundle of the basal deep brain, the ansa lenticularis (Supplementary Material 1: glossary). The fascicles related to those of the diencephalic-mesencephalic junction, whether they are anatomic neighbouring fibres or fibres embedded in the junction are also described.

3.1. Subthlamus and internal capsule

3.1.1. The cerebellorubral group

Brachium conjonctivum fibres went mainly to the capsule of the red nucleus and the ventrolateral thalamus via the commissure of Wernekink ("horse shoe commissure"). Most of medial brachium conjonctivum fibres bridged the two superior cerebellar peduncles (bridging crossed fibres) rather than decussating from one side to another (decussating crossed fibres), whereas the lateral fibres often did not cross the midline (uncrossed fibres) (Fig. 1). The fibres of red nucleus core were connected mainly with the ventrolateral thalamus through the pre-lemniscal radiations (Supplementary Material 1: glossary).

3.1.2. The reticulo-dorsal group

The ventral fibres of the reticulo-dorsal group were condensed along the midline (few crossing fibres) forming the ventral tegmental decussation of Forel (Fig. 2); superiorly they reached the inferior division of the ansa lenticularis and frontal projections. The central tegmental tract, longitudinal medial fascicle and basal forebrain bundle (BFB; Supplementary Material 1: glossary) were identified more dorsally following the curvature of the region (Fig. 2).

3.1.3. The tegmento-peripheral group

At the periphery of tegmentum (Supplementary Material 1:glossary), we defined two systems (partially overlapped) the anteromedial and posterolateral (Fig. 3). The anteromedial consisted of:

- the inferior division of the ansa lenticularis;
- frontal fibres, the most anterior and medial fibres forming the oblique fascicle;
- some of the lemniscal fibres;
- the so-called aberrant pyramidal fibres (Supplementary Material 1: glossary).

The posterolateral system consisted of: fibres of the posterior limb of the internal capsule, some passing through the subthalamic nucleus (STN) and the substantia nigra (SN); and most of lemniscal fibres. The two systems, along with thalamus-related fibres (see below), were included in the Forel's fields (Supplementary Material 1: glossary) and in the substance Q region (Schaltenbrand and Bailey, 1959).

3.1.4. The anterior limb of the internal capsule

Fronto-thalamic fibres projected to the anterior, medial and dorsal thalamic nuclei. We noticed that fronto-thalamic fibres formed a fronto-pulvinar fascicle (not described classically in humans), located superiorly, travelling through the stratum zonale (Fig. 4). Fronto-tegmental and ansa lenticularis fibres were intermingled in the medial and superior region of the cerebral peduncles. The inferior fibres of the anterior limb joined the genu of the internal capsule.

3.1.5. The posterior limb of the internal capsule

This limb contained mainly extrapyramidal projection fibres to the thalamus, subthalamus, tegmentum and pons. The pontine fibres followed a classic organization (Fig. 5). The superior thalamic radiations tracked from the ventral thalamus (Fig. 6) were organized according to the subcompartmentalization of thalamus (Morel et al., 1997). The ventral anterior region projected fibres to the frontal lobe through the superior thalamic peduncle and

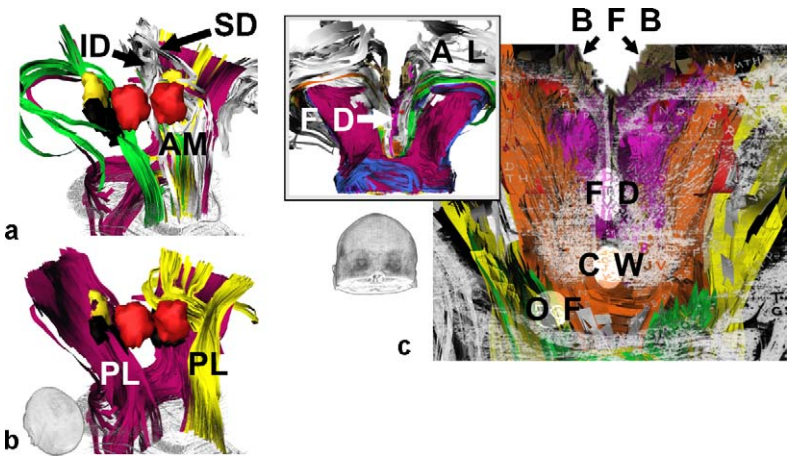

Fig. 3. The tegmento-peripheral group of subthalamic fibres (subject no. 4): a: the anteromedial system (AM) with the superior (SD) and inferior (ID) ansa lenticularis divisions, ventral lemniscal fibres (yellow), fibres of the internal capsule (purple) and the medial-most fibres of AM which form the oblique fascicle (green); b: the posterolateral system (PL) with fibres of the posterior limb of the internal capsule (purple, on the left) and lemniscal fibres (yellow, on the right); c: front view of a coronal section (registered with Riley (1953) with the commissure of Wernekink (CW), ventral tegmental decussation of Forel (FD), basal forebrain bundle (BFB), oblique fascicle (OF) and ansa lenticularis (inset, 3D front view with the peduncular projection fibres in purple).

Groupe tegmento-périphérique des fibres sous-thalamiques (sujet no. 4) : a : système antéro-médial (AM) avec les divisions supérieures (SD) et inférieures (ID) de l'anse lenticulaire, fibres lemniscales ventrales (jaune), fibres de la capsule interne (violet) et les fibres les plus médiales de AM formant le faisceau oblique (vert) ; b : système postéro-latéral (PL) avec des fibres du bras postérieur de la capsule interne (violet, à gauche) et des fibres lemniscales (jaune, à droite) ; c : vue frontale d'une coupe coronale (correspondance avec Riley (1953)) avec la commissure de Wernekink (CW), la décussation ventrale tegmentale de Forel (FD), le faisceau basal du cerveau antérieur (BFB), le faisceau oblique (OF) et l'anse lenticulaire (encart, vue frontale 3D avec les fibres pédonculaires de projection en violet).

the superior thalamic radiations; inferiorly fibres joined the ansa lenticularis and the reticulo-dorsal group (passing through H1 and H2 Forel's fields). The ventral lateral region projected cortical fibres through the superior thalamic radiations; inferiorly fibres joined the reticulo-dorsal and tegmento-peripheral groups and pontine fibres. The parafascicular nucleus–related region projected fibres to the fontal lobe and the ansa lenticularis, and posteriorly to the reticulo-dorsal group and the posterior commissure. The centromedian-related region mainly projected fibres to the central tegmental tract and few fibres to the tegmento-peripheral group. The pulvinar region projected fibres to the fronto-pulvinar fascicle, the temporo-thalamic fascicle of Arnold, ansa lenticularis, optical radiations (OR) and the supraoptic commissures (Supplementary Material 1: glossary). Cortico-subthalamic fibres were intermingled with the superior thalamic radiations (Fig. 6).

3.1.6. The sublenticular segment of the internal capsule

This segment can be separated in two regions, the anterior where the anterior commissure fibres spread, and the posterior or classical sublenticular region (Fig. 7). The posterior contained:

- ansa lenticularis fibres subdivided into two divisions, superior and inferior, respectively linked with the ventral and dorsal tegmentum;
- the temporo-thalamic fascicle of Arnold. In contrast to the ansa lenticularis, the ansa peduncularis is a poorly defined structure (Supplementary Material 1: glossary) and it was impossible to identify each component.

3.1.7. The retrolenticular segment of the internal capsule

This segment included various fibres (related to the temporal and occipital lobes, the posterior (dorsal) thalamus, lateral mesencephalon and ansa lenticularis) organized in a complex manner, intertwined with each other. Fibres tracked from the retrolenticular region (Supplementary Material 1: glossary), recognizable on color-coded images, were subdivided into three zones according to the direction of fibres (Fig. 8). These three zones, medial, dorsal, and lateral, included respectively: the optic system; the fronto-pulvinar fascicle; the major forceps, inferior fronto-occipital fascicle and tapetum (TAP; Supplementary Material 1: glossary). OR and Meyer's loop (Supplementary Material 1: glossary) intermingled with TAP fibres and reached the medial occipital lobe. The OR included a number of different fibres from the optic system (geniculo- and pulvinar-occipital fibres), longitudinal pathways, TAP, fascicle of Türck and ansa lenticularis. The fascicle of Türck comprised occipital and temporal fibres as well as ansa lenticularis fibres (Fig. 8).

3.2. Fascicles related to those of the diencephalic-mesencephalic junction

3.2.1. Longitudinal telencephalic pathways

The inferior intra hemispheric association pathways (Fig. 9) were identified in the lateral (external plus extreme) capsules and temporal stem. The inferior longitudinal fascicle and uncinate fascicle, as well as frontal and temporal U-shaped fibres were found in the lateral capsules, whereas the temporo-occipital fascicle, temporal and occipital U-shaped fibres, uncinate and arcuate fibres, and sublenticular fibres (ansa lenticularis, fascicle of Türck and temporo-thalamic fascicle of Arnold) were identified in the temporal stem. The temporo-occipital fascicle and inferior longitudinal fascicle intermingled in the occipital lobe.

3.2.2. Commissural fascicles between the cerebral hemispheres

The genu (beak) forepart of the corpus callosum contained fibres related to the medial and basal orbitofrontal cortices (Fig. 10). Tapetum was tracked from the paraventricular and retrolenticular regions. The distribution of these fibres was not described classically. Tapetal fibres were connected to the occipital, temporal and frontal lobes, as well as the pulvinar and the lateral mesencephalon – where they mingle with the fascicle of Türck (Fig. 10). The two columns of the fornix were identified with their pre- and post-commissural (anterior commissure, AC) contingents (Fig. 10). AC and posterior commissure (PC) were studied with the sublenticular and subthalamic regions, respectively. The different components of the supraoptic commissures, which are poorly described in man (Riley, 1953), were not clearly identified. However, we found vertical fibres crossing from the pallidum to the

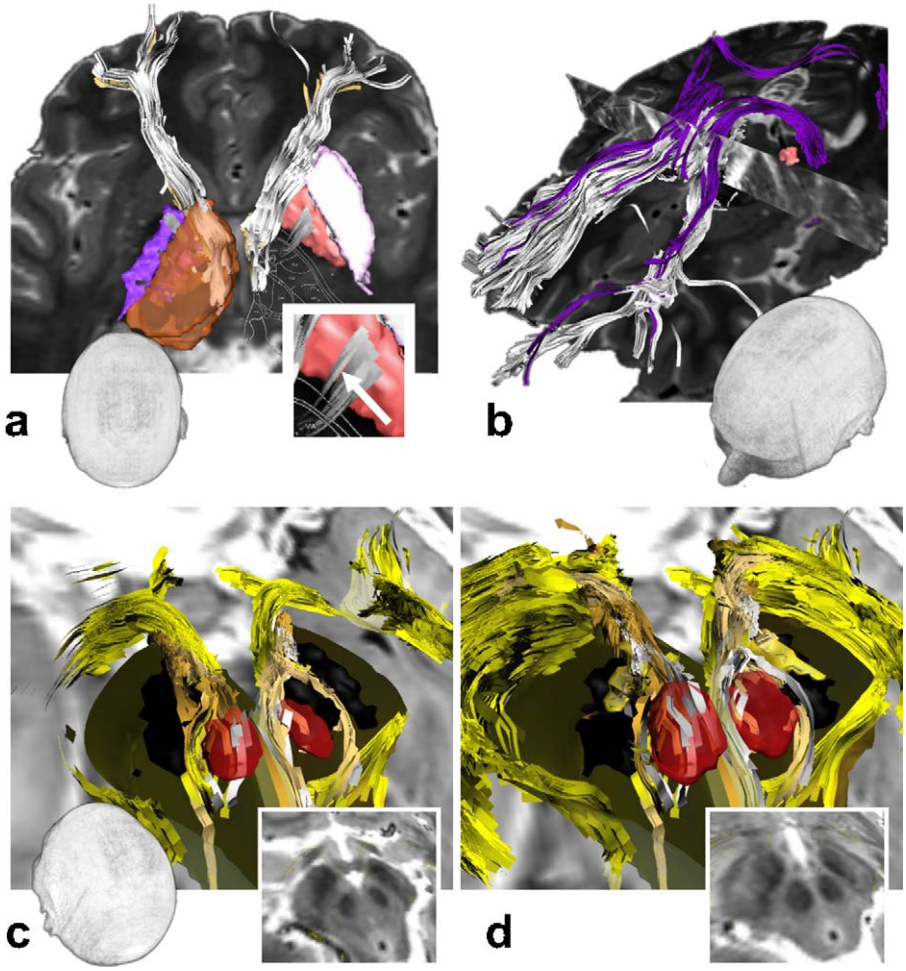

Fig. 4. Anterior limb of the internal capsule: a: anterior limb (white) and genu (gold) fibres (subject no. 1), extrapyramidal fibres reaching the posterior limb are also visible (arrows) (the whole posterior limb is displayed in purple on one side); b: fronto-pulvinar fascicle (purple) (subject no.1); c,d: fibres located in the antero-medial region of the cerebral peduncle (subject no. 2), horizontal sections, where ansa lenticularis (yellow) and frontal (white and gold) fascicles intermingle (section C is below section D).
Bras antérieur de la capsule interne : a : fibres (sujet no. 1) du bras antérieur (blanc) et du genou (doré), des fibres extrapyramidales atteignant le bras postérieur sont aussi visibles (flèches) (l'ensemble du bras postérieur est représenté en violet sur un côté) ; b : faisceau fronto-pulvinar (violet) (sujet no.1) ; c,d : fibres localisées dans la région antéro-médiale du pédoncule cérébral (sujet no. 2), coupes horizontales, où l'anse lenticulaire (jaune) et des faisceaux frontaux (blanc et doré) se mélangent (la coupe C est au dessous de la coupe D).

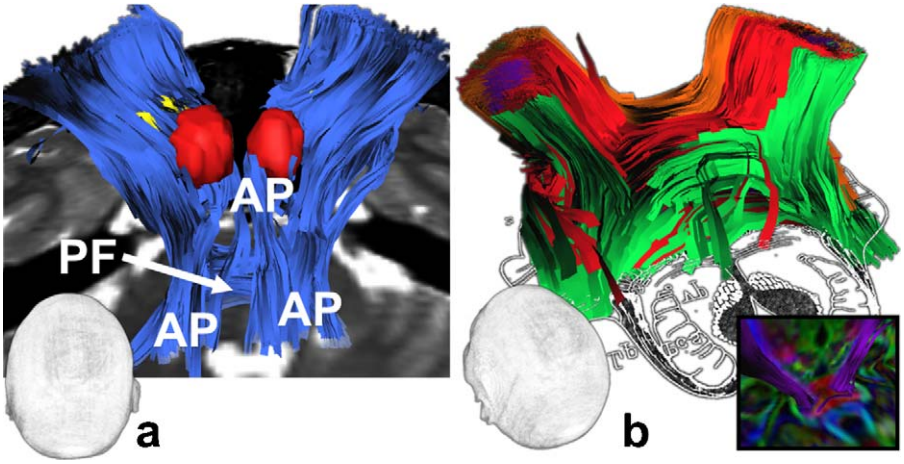

Fig. 5. Posterior limb of the internal capsule, brain stem fibres: a: pontine (PF) and aberrant pyramidal fibres (AP) (subject no. 1); b: the PF group comprise (subject no. 5): (i) pyramidal (cortico- pontine and spinal) contingent through the pontine nuclei area (purple, inset depicts nuclear-related fibres only), (ii) crossing fibres (red), (iii) anterior peduncular fibres (orange), and (iv) posterolateral fibres of the middle cerebellar peduncle (green; brachium pontis).
Bras postérieur de la capsule interne, fibres du tronc cérébral : a : fibres (sujet no. 1) pontines (PF) et pyramidales aberrantes (AP) ; b : le groupe PF comprend (sujet no. 5) : (i) un contingent pyramidal (cortico-pontin et spinal) traversant la région des noyaux du pont (violet ; dans l'encart seules des fibres nucléaires sont représentées), (ii) des fibres croisées (rouge), (iii) des fibres pédonculaires antérieures (orange), et (iv) des fibres postéro-latérales du pédoncule cérébelleux moyen (vert ; brachium pontis).

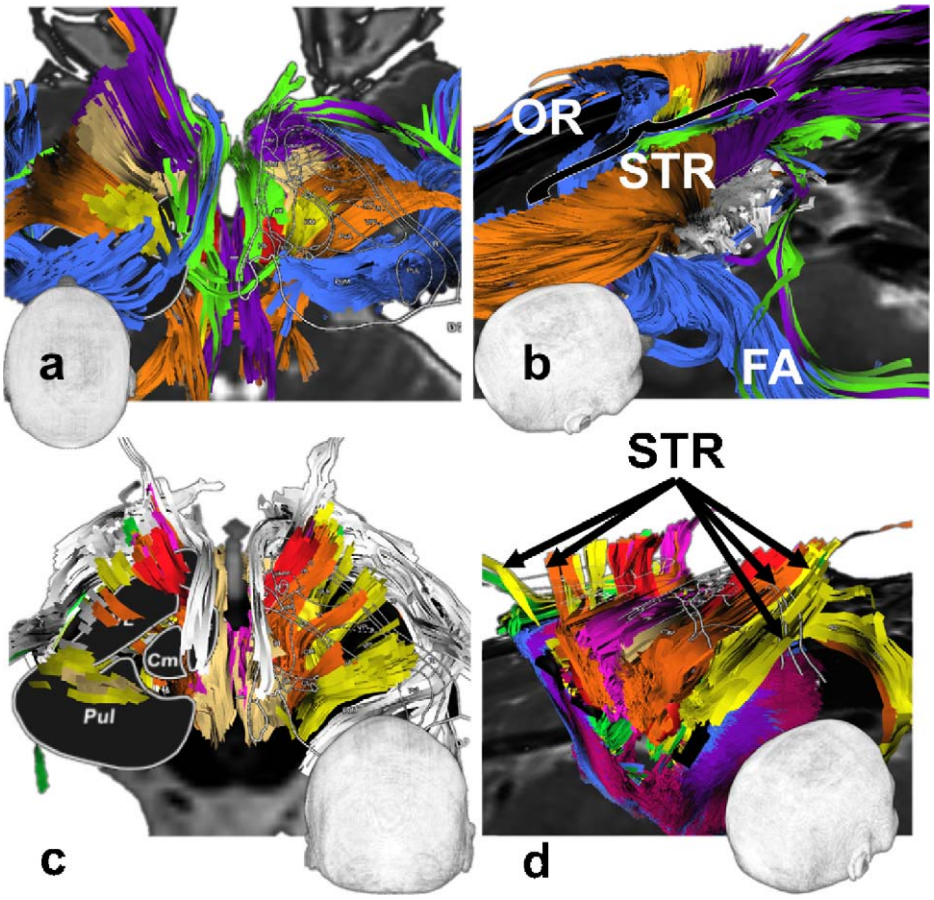

Fig. 6. Posterior limb of the internal capsule (registration with the slice 3 mm above the horizontal AC-PC plan (Morel et al., 1997)); a: thalamic fibres of the superior thalamic radiations (subject no. 1): ventral anterior (purple), ventral median (gold), ventral lateral (orange), center median (yellow), para fascicularis (green) and pulvinar (blue) contingents; b: thalamic fibres of the superior thalamic radiations (STR) (subject no. 1): projection fibres (white) are cut horizontally at the upper brainstem, the fascicle of Arnold (FA) and the optic radiations (OR) are visible; c: cortico-subthalamic fibres (subject no. 4): cerebellorubral group (orange); mammillothalamic bundle (red); ansa lenticularis -related fibres (white); lemniscal-related fibres (yellow) and reticulo-dorsal group (beige and pink); d: cortico-subthalamic fibres (subject no. 4): relationships with the superior thalamic radiations (STR) within the posterior limb (coronal section along red nucleus-related fibres).
Bras postérieur de la capsule interne (correspondance avec la coupe 3 mm au dessus du plan horizontal AC-PC (Morel et al., 1997)) : a : fibres thalamiques des radiations thalamiques supérieures (sujet no. 1) : contingents, ventral antérieur (violet), ventral médian (doré), ventral latéral (orange), central médian (jaune), para fasciculaire (vert) and pulvinarien (bleue); b : fibres thalamiques des radiations thalamiques supérieures (STR) (sujet no. 1) : des fibres de projection (blanc) sont sectionnées horizontalement au niveau de la partie haute du tronc cérébral, le faisceau d'Arnold (FA) et les radiations optiques (OR) sont visibles ; c : fibres cortico-sous-thalamiques (sujet no. 4) : groupe cérébello-rubral (orange) ; faisceau mamillo-thalamique (rouge) ; fibres de l'anse lenticulaire (blanc) ; fibres du lemnisque médian (jaune) and groupe réticulo-dorsal (beige et rose) ; d : fibres cortico-sous-thalamiques (sujet no. 4) : relations avec les radiations thalamiques supérieures (STR) dans le bras postérieur (coupe coronale le long des fibres du noyau rouge).

optic tract that might be related to this commissural network (Fig. 10).

3.2.3. Radiate fibres

The radiate fibres were explored in each region (tracked from the caudate nucleus, putamen, pallidum, thalamus, subthalamic nucleus and substantia nigra). We only found:

- inferior (basal) pallidal fibres joining the ansa lenticularis and AC that were often intermingled with the supraoptic commissure fibres;
- short caudate fibres that joined the anterior limb of the internal capsule;
- short intra putaminal fibres.

3.2.4. Nucleus-related subthalamic fibres

Nucleus-related fibres (Fig. 11) form an inhomogeneous group characterized by gray matter tracking (for red nucleus-related fibres: see manuscript). The tegmental pedunculopontine nucleus-related fibres reached the intralaminar thalamus and mingled with the central tegmental tract, whereas others reached rubral bundles. The subthalamic nucleus-related fibres reached the superior thalamic radiations, the ansa lenticularis and the reticulo-dorsal group. The substantia nigra-related fibres reached the frontal superior thalamic radiations and the pontine fibres. Finally, fibres linked with substance Q were intermingled with the tegmento-peripheral group.

3.2.5. Inter-subject variability

The same observers performed the analysis on the six subjects; globally, the same connectivity patterns were identifiable. However, we noticed several differences (subjective analysis; not quantified) in term of fascicle thickness. The relative thickness of fascicles belonging to the same region, were different from one subject to another:

- within the retrolenticular region, between the TAP and fascicle of Türck, the posterior fibres of AC and ansa lenticularis and the inferior longitudinal pathways;
- within the medial, anterior and superior region of brain peduncles, between the ansa lenticularis, the anterior (and genu) and the posterior limbs of the internal capsule;

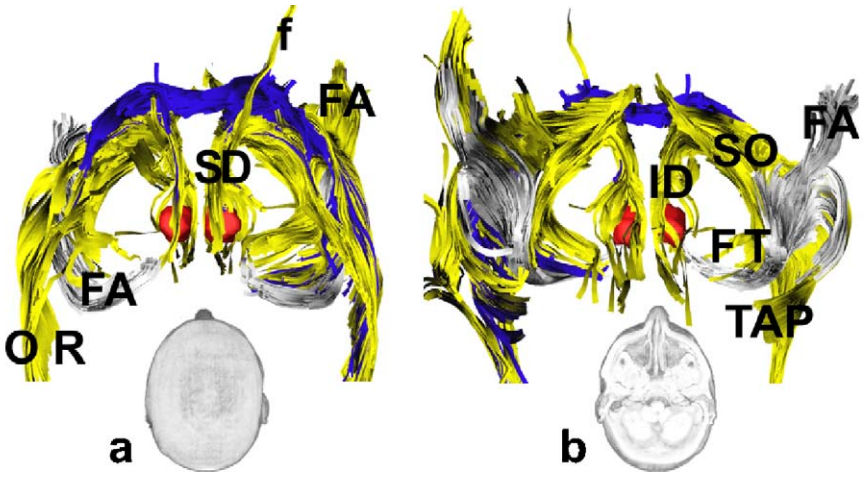

Fig. 7. Sublenticular portion of the internal capsule (subject no. 5): a: superior; b: inferior, views: ansa lenticularis (yellow) with its superior (SD) and inferior (ID) divisions, along with anterior commissure (blue), temporo-thalamic fascicle of Arnold (FA), fascicle of Türck (FT), supraoptic commissure-related fibres (SO), optic radiations (OR) and tapetum (TAP) and fronto-tegmental projections (f).
Portion sous lenticulaire de la capsule interne (sujet no. 5). Vues a : supérieure; et b : inférieure : anse lenticulaire (jaune) avec ses divisions supérieure (SD) et inférieures (ID), commissure blanche antérieure (bleu), faisceau temporo-thalamique d'Arnold (FA), faisceau de Türck (FT), fibres des commissures supra-optiques (SO), radiations optiques (OR) et tapetum (TAP) et fibres de projection fronto-tegmentales (f).

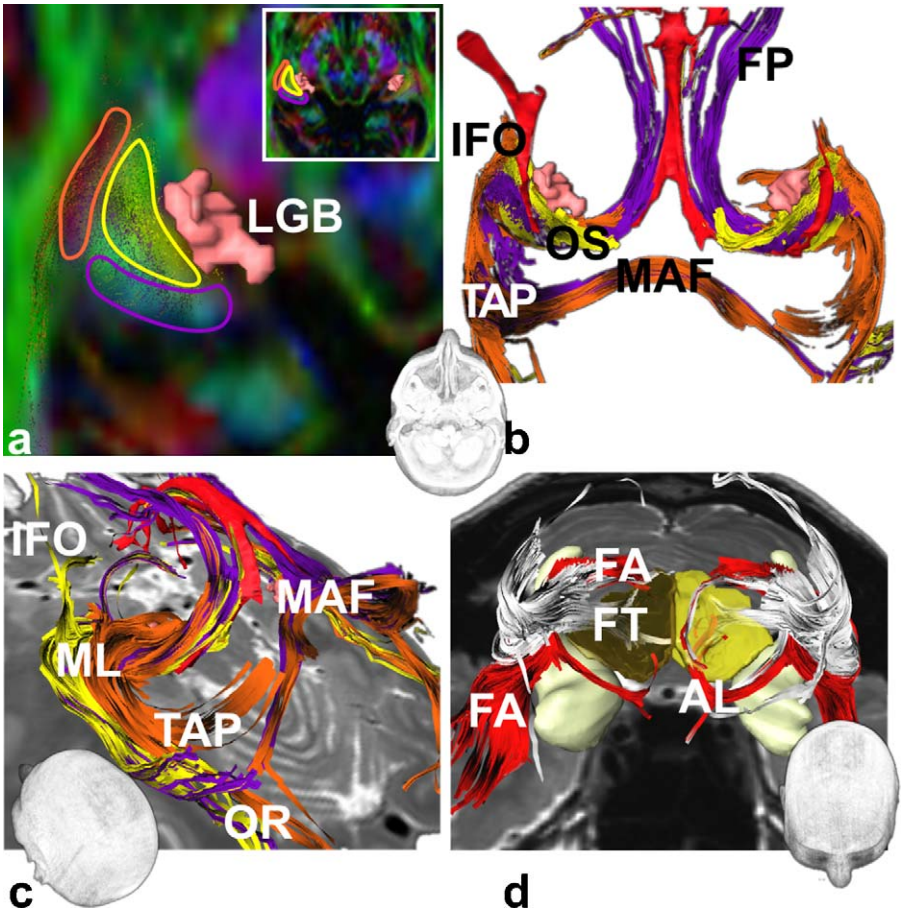

Fig. 8. Retrolenticular segment of the internal capsule: a: location of the retrolenticular region (LGB, lateral geniculate body), yellow, orange and purple ROIs defined on an axial colour-coded map (inset overview) (subject no. 2); b: fronto-pulvinar fascicle (FP), major forceps of corpus callosum (MAF), optic system (OS), inferior longitudinal fascicle (IFO) and tapetum (TAP), for information the trigone is displayed (red); c: optical radiations (OR) and Meyer's loop (ML) (subject no. 1); d: fascicle of Türck (FT) and fascicle of Arnold (FA).
Portion rétro-lenticulaire de la capsule interne ; a : localisation (sujet no. 2) de la région rétro-lenticulaire (LGB, corps géniculé latéral) avec 3 ROIs jaune, orange et violette, définies sur une carte de direction codée par couleur dans un plan axial (encart, vue d'ensemble) ; b : faisceau fronto-pulvinarien (FP), forceps major du corpus callosum (MAF), système optique (OS), faisceau longitudinal inférieur (IFO) et tapetum (TAP), le trigone est représenté pour information (rouge) ; c : radiations optiques (OR) et boucle de Meyer (ML) (sujet n° 1) ; d : faisceau de Türck (FT) et faisceau d'Arnold (FA).

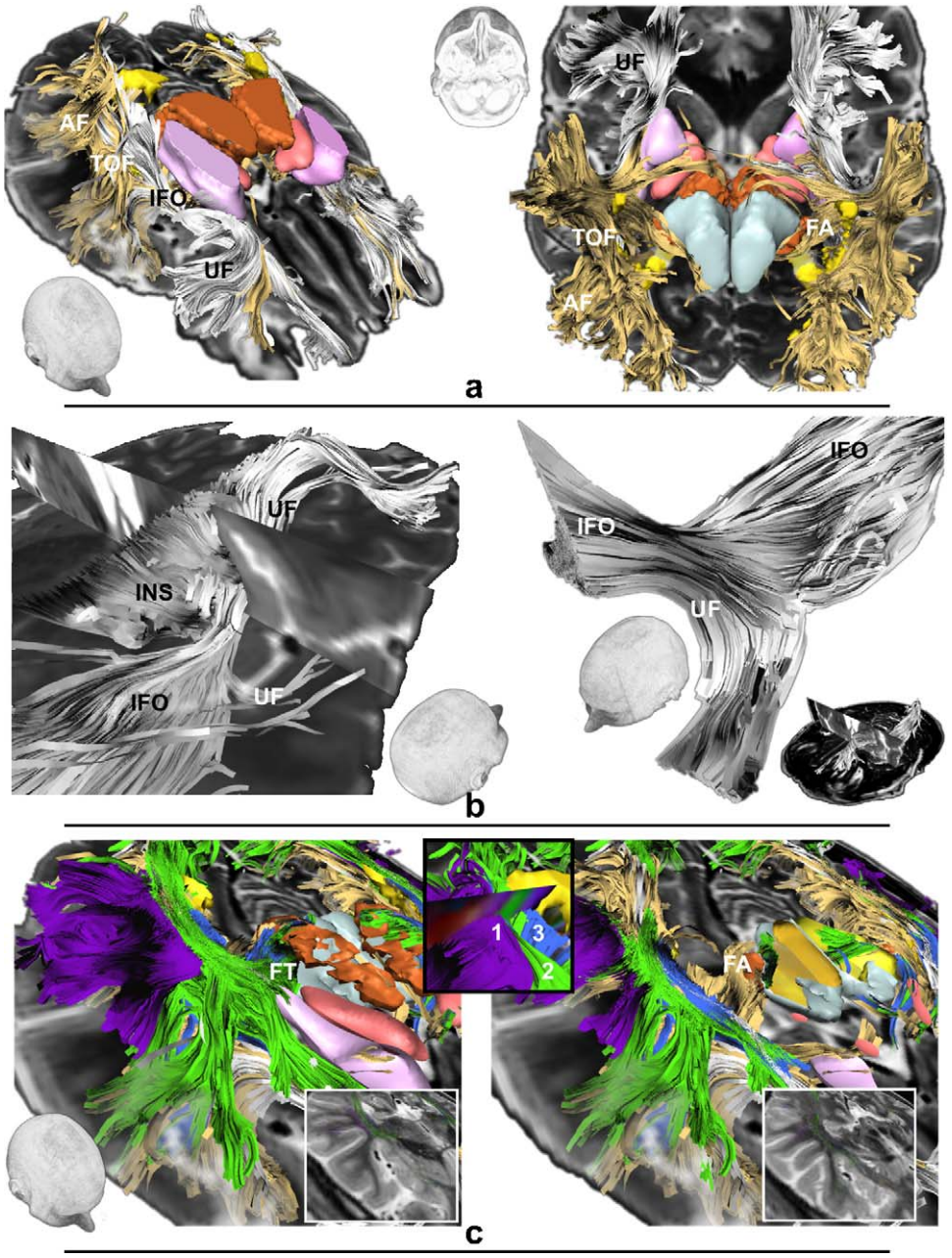

Fig. 9. Telencephalic longitudinal pathways (TLPs) and related fascicles: Türck's (FT), Arnold's (FA), and insular (INS): a: TLPs: (1) tracks of the lateral capsules (Subject no. 1) are shown in white, the U-shaped fibres, the uncinate fascicle (UF) and the inferior fronto-occipital fascicle (IFO); fascicles of the temporal stem are shown in gold, the temporo-occipital fascicle (TOF), U-shaped fibres and the arcuate fascicle (AF); b: the relationship between the IFO, INS and UF is depicted (left, subject no. 2; right, subject no. 3); c: Layers of fibres facing the ventricular trigone (Subject no. 1): [1] superficial temporal fibres; [2] intermediate fibres, mainly IFO plus TOF fibres, and rare tapetal fibres (blue); and [3] deep tapetal fibres.
Voies longitudinales télencéphaliques (TLPs) et faisceaux en rapport : faisceaux de Türck (FT), d'Arnold (FA) et insulaire (INS) : a : TLPs : (1) fibres des capsules latérales (sujet no. 1) en blanc, fibres en U, faisceau unciné (UF) et faisceau fronto-occipital inférieur (IFO) ; faisceaux du lobe temporal en doré, faisceau temporo-occipital (TOF), fibres en U et faisceau arqué (AF) ; b : Relations entre IFO, INS and UF (gauche, sujet no. 2 ; droite, sujet no. 3) ; c : Couches de fibres en regard du carrefour ventriculaire (sujet no. 1) : [1] fibres superficielles temporales [2], fibres intermédiaires, principalement des fibres du IFO et du TOF, et quelques fibres du tapetum (bleu) ; et [3] des fibres profondes du tapetum.

- within the lateral subthalamus, between the lemniscal and aberrant pyramidal fibres;
- within the cerebellorubral route, between crossed and uncrossed (commissure of Wernekink) fibres;
- within the pulvinar, between fronto-pulvinar fibres, the OR and temporo-thalamic fascicle of Arnold.

The small commissure of Forel was identified in two of six cases (Fig. 10). The radiate fibres (Supplementary Material 1: glossary) were rarely identifiable except below the pallidum.

4. Discussion

We analysed in explicit details the 3D WM architecture of the deep brain using high resolution DTI and deterministic fibre tracking. Interplay between anatomy textbooks and our data, visualized on 2D slices and on 3D reconstructions in the volume-rendered brain, allowed us to iteratively refine the fibre tracking of each individual fascicle. This test-re-test approach (back and forth between fibre tracking and anatomic analysis), while subjective and qualitative, was nonetheless very informative. We visualized

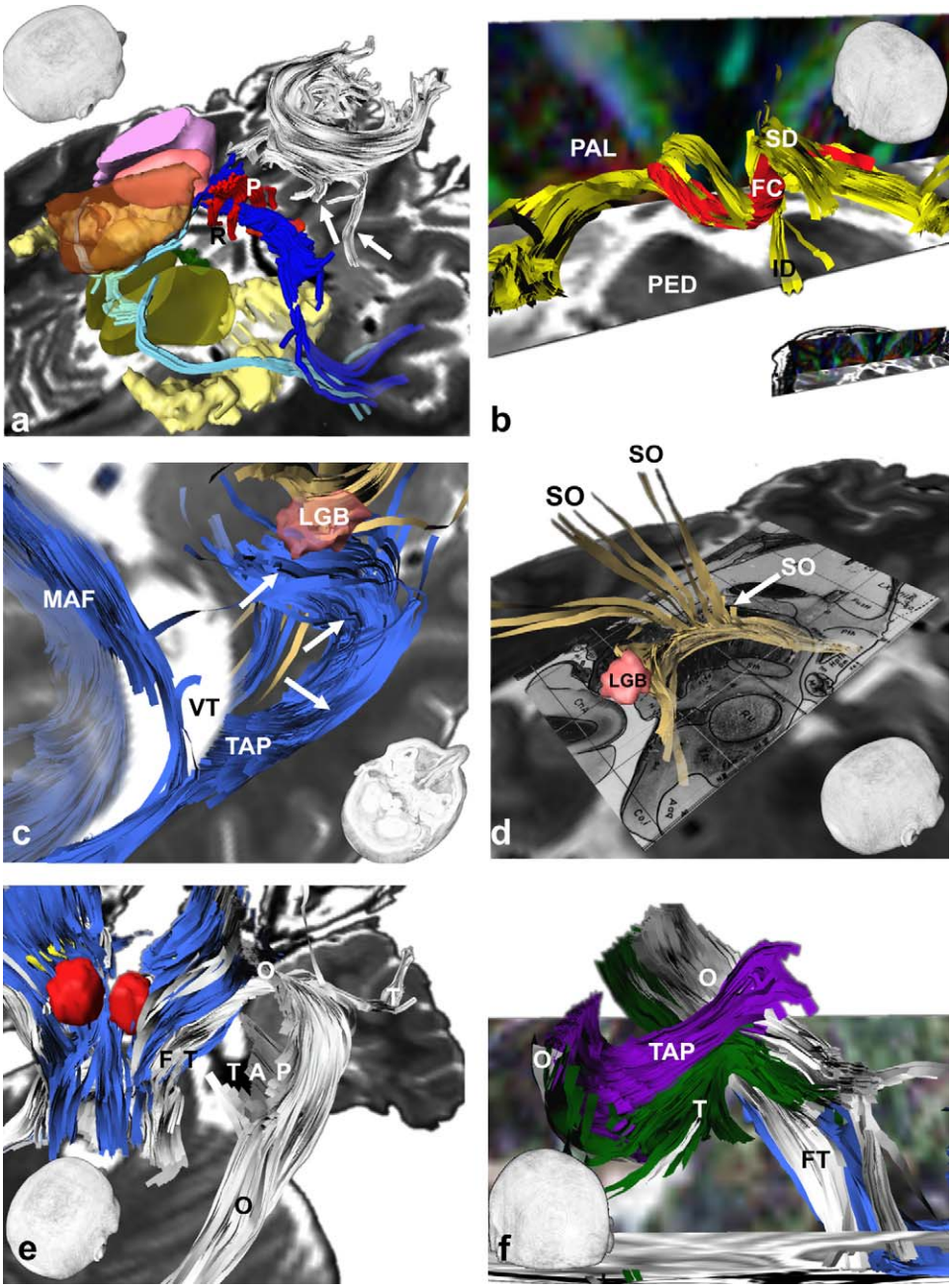

Fig. 10. Commissural (and related) fascicles between the cerebral hemispheres (from A to F, subjects no. 1, 3, 2, 1, 2 and 6): a: the minor forceps (white; orbitofrontal fibres through the beak, arrows), AC (blue), PC (pale blue) and trigonal fibres (pre- (P) and retro- (R) commissural contingents, red; b: commissure of Forel (FC) with the superior (SD) and inferior (ID) divisions of the ansa lenticularis (pallidum, PAL; peduncle, PED); c: major forceps (MAF) and tapetum (TAP) (white arrows) facing the ventricular trigone (VT) that reaches the posterior thalamus (LGB, lateral geniculate body; optic tract, gold) and the MAF; d: shown are the supposed (see text) supraoptic commissure-related fibres (SO); e: fascicle of Türck (FT), tapetum (TAP) plus temporal (T) and occipital (O) fibres, pontine fibres (white) and fibres of the posterior limb (blue). f. T (green), O (white) and TAP (purple) fibres.

Faisceaux commissuraux (et ceux en rapport) entre les hémisphères cérébraux (de A à F, sujets no. 1, 3, 2, 1, 2 et 6) : a : forceps mineur (blanc ; fibres orbito-frontales passant par le bec, flèches), AC (bleu), PC (bleu pâle) et fibres du trigones (contingents pré- (P) and rétro- (R) commissuraux, rouge ; b : commissure de Forel (FC) avec les divisions supérieure (SD) et inférieures (ID) de l'anse lenticulaire (pallidum, PAL ; pédoncule, PED) ; c : forceps majeur (MAF) et tapetum (TAP) (flèches blanches) en regard du carrefour ventriculaire (VT) qui rejoignent le thalamus postérieur (LGB, corps géniculé latéral ; voie optique, doré) et MAF ; d : fibres en lien avec les commissures supra-optiques (voir texte) (SO) ; e : faisceau de Türck (FT), tapetum (TAP) et fibres temporales (T) et occipitales (O), fibres du pont (blanc) et fibres du bras postérieur (bleu) ; f : fibres T (vert), O (blanc) et du TAP (violet).

and detailed most of the deep WM bundles described by pioneering neuroanatomists including large and complex fascicles such as the basal forebrain bundle and the ansa lenticularis. This modern in vivo analysis leads to important insight into the 3D organization of this complex WM architecture. Our findings lent to propose a topographic classification of subthalamic fascicles into three groups (Supplementary Material 5, which shows the overview of the whole organisation of deep brain WM fascicles): the cerebellorubral, the reticulo-dorsal and the tegmento-peripheral one.

4.1. Diffusion tensor imaging and fibre tracking analysis

With an optimised sequence, limited coverage, and a relatively long yet clinically acceptable scanning time, we reached a voxel volume of $1.25 \times 1.25 \times 1.5\ mm^3$. This is less than half the volume used

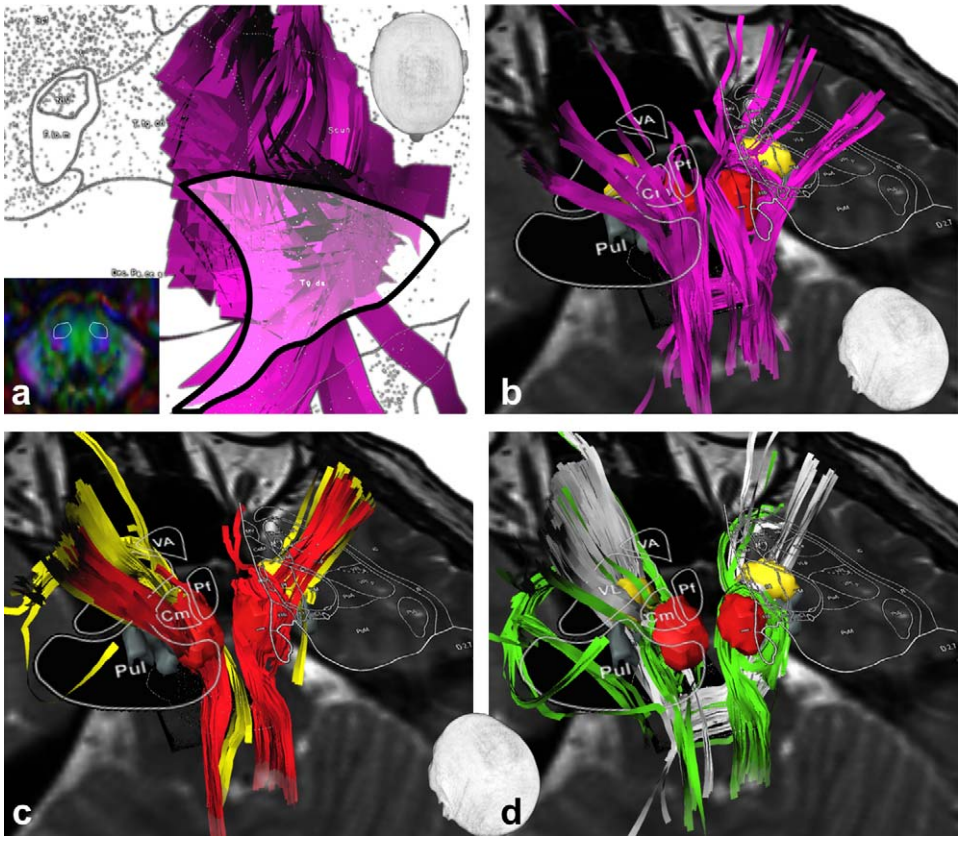

Fig. 11. Nucleus-related fibres (subject no. 1): a: pedunculopontine nucleus ROI superimposed on Olszewski and Baxter (1954)'s atlas (bold dark line); inset left and right ROIs (white circles) on colour-coded image; b: pedunculopontine nucleus-related fibres (pink); c,d: red nucleus-(red), subthalamus- (yellow), SN- (white) and substance Q (green)-related fibres.
Fibres issues des noyaux (sujet no. 1) : a : ROI du noyau pédonculo-pontin tegmental localisée sur l'atlas d'Olszewski et Baxter (1954) (trait noir épais) et en encart ROIs droite et gauche (cercles blancs, tegmentum droit et gauche) sur une carte de direction codée par couleur dans un plan axial ; b : fibres issues du noyau pédonculo-pontin tegmental (rose) ; c,d : fibres issues du noyau rouge (rouge), du noyau sous-thalamique (jaune), de la substance noire (blanc) et de la substance Q (vert).

in other DTI studies of the same region (Habas and Cabanis, 2007; Nagae-Poetscher et al., 2004), but we maintained an equivalent or superior signal-to-noise ratio. This enabled us to study fascicles from 2 to 7 mm diameter (Supplementary Material 6, which gives the rough diameter of small fascicles).

DTI images are acquired with an echo-planar imaging sequence, which is prone to susceptibility artifacts. The use of parallel imaging (sensitivity encoding) (Jaermann et al., 2004) minimized these artifacts. However, at the current state of technology they cannot be totally avoided. In our study, this phenomenon disturbed fibre tracking on a case-by-case basis in two ways: artifacts of the ventral pons and distortion of colour-coded maps in the fronto-callosal region. The former precluded tracking in the ventral pons; whereas the latter was taken into account when comparing T2 versus DTI images (anatomic landmarks were useful, like those contoured). Movement artifacts also decrease image quality, especially at high resolution; however they should have been limited by the vacuum cushion used in this study.

The direct identification of the entire length of deep fascicles is generally not possible on colour-coded maps because of the complex structural anatomy at the diencephalo-mesencephalic junction. The understanding of 3D organization of WM fascicles afforded by our study shows that at a macroscopic level it is however possible to identify certain fascicles when they cross the axial plane (Fig. 12). This is more complex when fascicles interweave, a problem which is well known at the infra millimeter level when different fibres (i.e. axons) cross in the same voxel (Oouchi et al., 2007; Tuch et al., 2003). However the difficulty to identify very small fibres, kissing or crossing, was minimized in our macroscopic study by using small voxels while seeking only supra millimetre diameter connectivity (Supplementary Material 6, which gives the rough diameter of small fascicles). Nevertheless, the problematic of the differentiation of kissing and crossing fibre is still a limitation of anatomical studies based on deterministic DTI fibre tracking, including our study. Partial biologic and anatomic knowledge of human brain fascicles added with still on-going research on mathematical models used for the display of fascicles preclude any firm and definitive conclusion about the detailed biologic organization hidden behind DTI fibre tracking technique. This challenge fosters the research of new methodologies (Leow et al., 2009).

Finally, even though averaging and spatial normalization of the DTI datasets into a standard atlas (Jones et al., 2002) could have been a useful statistical tool to confirm the repeatability of our results; it would have also reduced the benefits of the high resolution of individual datasets and made the tracking of small WM fascicles described in this study likely impossible. This approach would certainly be interesting in the future in parallel with clinically useful individual subject analysis studies.

4.2. Analysis of white matter fascicles

Our results using in vivo technique give new topographic insights into this complex region.

Within the subthalamus, our findings highlight the ambiguity concerning the crossing of the cerebellorubral paths (Dejerine, 1901; Laget, 1973; Nieuwenhuys et al., 1979; Olszewski and Baxter,

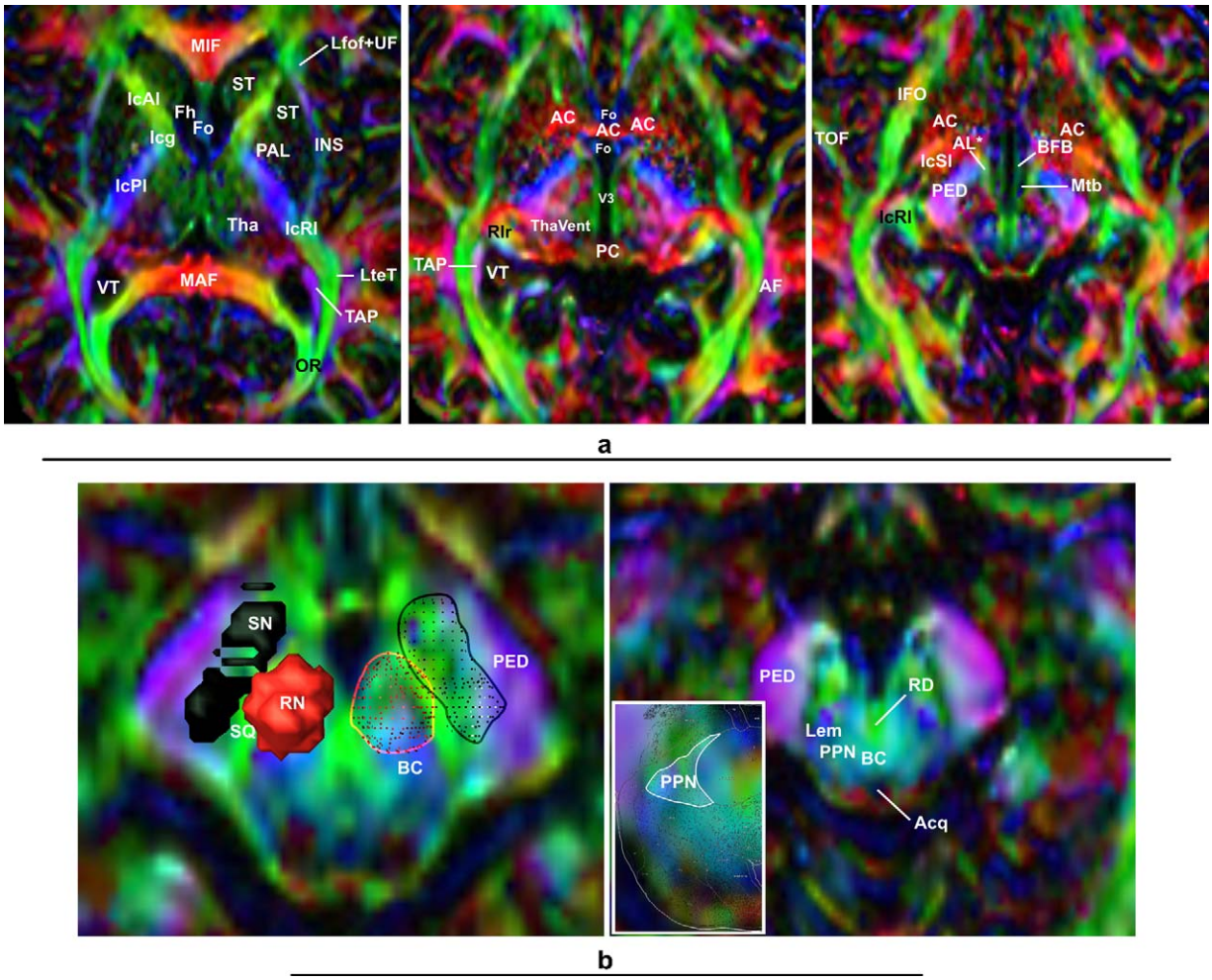

Fig. 12. Analysis of axial colour-coded map: a: locations of bundles are shown from superior (left) to inferior (right) plans; b: locations of ROIs for the grey matter analysis: the projection of 3D structures is on the left, along with the red nucleus (RN) and substantia nigra (SN), the projection of the pedunculopontine nucleus (tegmental, PPN) is on the right, a colour-coded map reconstructed along a section of Olszewski and Baxter (1954)'s atlas is presented in the inset. Abbreviations: AC, anterior commissure; Acq, aqueduct of the brain; AF, Arcuate fascicle; AL*, Ansa lenticularis located outside the sublenticular region; BC, Brachium conjunctivum; MAF, MIF, forceps major (MA) and minor (MI) of the corpus callosum; Fo, Fornix; Fh, Frontal horn of the lateral ventricle; IcAl, Internal capsule (IC), anterior limb; Icg, IC, genu; IcPl, IC, posterior limb; IcRl, IC, retro-lenticular region; IcSl, IC, sub-lenticular region; IFO, Inferior fronto-occipital fascicle; INS, Insular fascicles; Lem, Lemniscus; Lfof + UF, Longitudinal fronto-occipital fascicle plus uncinate fascicle; LteT, Longitudinal telencephalic tracts; BFB, Basal forebrain bundle; Mtb, Mamillothalamic bundle; OR, Optic radiations (broad meaning; see text); PAL, Pallidum; PC, Posterior commissure; PED, Peduncular bundles; PPN, Pedunculopontine nucleus (Tegmental); RD, Reticulo dorsal group (see text); RIr, Retrolenticular region; RN, Red nucleus; SQ, Substance Q; SN, Substantia nigra; ST, Striatum (caudate nucleus and putamen); TAP, Tapetum; TOF, Temporo-occipital fascicle; Tha, Thalamus; ThaVent, Ventral region of the thalamus; VT, Trigone of the lateral ventricle; V3, Third ventricle.

Analyse de carte de direction codée par couleur dans un plan axial : a : localisations des faisceaux de la partie supérieure (gauche) à la partie inférieure (droite) du cerveau ; b : localisations des ROIs pour l'analyse de la substance grise : à gauche, projection des structures 3D, passant par le noyau rouge (RN) et la substance noire (SN) ; à droite, projection du noyau pédunculo-pontin tegmental (PPN) avec en encart une carte de direction codée par couleur reconstruite dans un plan passant par la coupe de l'atlas d'Olszewski et Baxter (1954). Abréviations : AC, commissure blanche antérieure ; Acq, aqueduc du cerveau ; AF, faisceau arqué ; AL, anse lenticulaire localisée hors de la région sous lenticulaire ; BC, Brachium conjunctivum ; MAF, MIF, forceps majeur (MA) et mineur (MI) du corps calleux ; Fo, fornix ; Fh, corne ventriculaire frontale ; IcAl, bras antérieur de la capsule interne (IC) ; Icg, genou (IC) ; IcPl, bras postérieur (IC) ; IcRl, région rétro-lenticulaire (IC) ; IcSl, région sous-lenticulaire (IC) ; IFO, faisceau fronto-occipital ; INS, faisceaux insulaires ; Lem, lemnique ; Lfof + UF, faisceau longitudinal fronto-occipital et faisceau unciné ; LteT, faisceaux longitudinaux télencephaliques ; BFB, faisceau basal du cerveau antérieur ; Mtb, faisceau mamillo-thalamique ; OR, radiations optiques (au sens large ; voir texte) ; PAL, pallidum ; PC, commissure blanche postérieure ; PED,faisceaux pédonculaires ; PPN, noyau pédonculo-pontin tegmental ; RD, groupe réticulo-dorsal (voir texte) ; RIr, région rétro-lenticulaire ; RN, noyau rouge ; SQ, substance Q ; SN, substance noire ; ST, striatum (noyau caudé et putamen) ; TAP, Tapetum ; TOF, faisceau temporo-occipital ; Tha, thalamus ; ThaVent, région ventral du thalamus ; VT, carrefour du ventricule latérale ; V3, troisième ventricule.*

1954; Riley, 1953), notably complicated by the intermingling of brachium conjonctivum fibres with tegmental fascicles (Fig. 1). All the published characteristics of human BFB fit with our results, allowing for the first time in vivo the description of the entire BFB (Fig. 2). The tegmento-peripheral group shows a double organization related to the reticular system, the cerebellorubral group, the ansa lenticularis and the lemniscuses.

Concerning the projection fibres of the internal capsule, we suggest the existence of a new fascicle, the fronto-pulvinar, connecting the frontal polar cortices with the pulvinar that was already described in monkeys (Petrides and Pandya, 2007). The projection fibres of the posterior limb appear to primarily consist of extrapyramidal fibres (the occipital and temporal cortices project through the retrolenticular region). The limited volume of imaged brain (36 mm thickness) prevented any firm conclusion concerning the detailed cortical connections of fibres passing through the posterior limb.

We found that the surface of the thalamus, wrapped laterally by thalamocortical fibres forming the superior thalamic radiations (passing through the reticular nucleus or Arnold's net), is also coated with other extrapyramidal projection fibres that pass through the subthalamus (Fig. 6). We also found a large bundle that fits the description by Dejerine (Dejerine, 1901) of a rich network of myelinated fibres connected with the subthalamic region (the region of "Ruban de Reil médian").

Within the sub- and retro-lenticular segments of internal capsule, our findings show the complexity of OR made of the geniculo-calcarine tract, TAP, fronto-occipital fascicle, temporo-occipital fascicle, uncinate fascicle, ansa lenticularis and fascicle of Türck (Fig. 8). This might explain the variability noticed with statistical anatomic approaches (Bürgel et al., 1999), and the over-estimation of the Meyer's loop (Yamamoto et al., 2005). The topography and organization of the ansa lenticularis is well defined, and for the first time totally revealed in vivo (Fig. 7).

The organization of the telencephalic longitudinal pathways and the neighboring uncinate fascicles described here is in agreement with the classic organization, as well as DTI fiber tracking of the arcuate fascicle and temporo-occipital fascicles (Catani et al., 2005).

We collected new information about the AC, PC and fornix. Notably, we visualized the pre- and post-commissural contingents of the fornix, the former being connected to the basal forebrain, namely the preoptic area (or prothalamus) on the Schaltenbrand & Bailey atlas (Schaltenbrand and Bailey, 1959). However, the complexity of this region (Heimer, 2000) does not permit any conclusions regarding a precise connection.

The TAP is a complex structure, inherited from topographic descriptive anatomy, which can be split into its different components: the temporo-occipital – the commonly accepted commissure between the temporal and occipital lobes; and a new connectivity, inter-thalamic (between the two pulvinars), towards the frontal lobes (through the inferior longitudinal fascicle) and the upper brainstem (dorso-laterally, mingled with the fascicle of Türck). The TAP and the others fibres facing the ventricular trigone are organized in three layers identifiable on DTI slices (Fig. 9).

Our study of radiate fibres did not provide detailed results, perhaps due to: the spreading of fibres through large isotropic bundles beyond the geometric resolution of our DTI tracking system (e.g., the stratum pedunculi); or the unknown connectivity of grey matter that might be hidden by mainstream WM tracking of neighbouring, or crossing, fascicles. It seems that our inability to track small fascicles (e.g., mamillo-peduncular and retroflexus fascicles), as well as the variable visibility of small structures (commissure of Forel), is linked to the limited geometric resolution of our DTI fibre tracking.

Concerning nucleus-related fibres, an important connection between the pedunculopontine nucleus and subthalamic nucleus using a probabilistic approach to balance the low accuracy of ROI positioning has been described (Aravamuthan et al., 2007) whereas our results, using individual-based approach, show limited connectivity (Fig. 11). The high density of fibres around the pedunculopontine nucleus embedded in the mesencephalic reticular formation (Nieuwenhuys et al., 1979; Olszewski and Baxter, 1954) could explain this discrepancy. This complexity, along with the lack of information about grey matter fibres, brings into question fine connectivity revealed by statistical approaches. Results of the other grey matter structures we explored (subthalamic nucleus, substantia nigra, and substance Q) illustrate the limits of grey matter tracking; the red nucleus is an exception because it (core and capsule) classically consists primarily of fibres (Dejerine, 1901).

Finally, the design of the study, the evaluation of the potential of DTI fiber tracking to explore and analyse the complexity of deep brain, did not allow quantifying the inter-subject variability. This could be done more easily after detailed descriptive explorations, like this work. Although subjective, we found morphologic differences in connectivity that may not predict of differences in functionality. Given the complexities of human neuroanatomy, such variability could be significant. The variations concerning small fascicles can be explained by technical limitations of our study and/or by true variability in the organization of WM bundles.

5. Conclusion

In conclusion, we charted in vivo most of the tracts described in the deep brain, including large and complex fascicles such as the basal forebrain bundle and the ansa lenticularis. In functional and minimally invasive neurosurgery, the possibility to map both grey and white matter structures deep inside the brain will have major implications. Today, the deposition of electricity in deep brain stimulation (Herzog et al., 2007), tomorrow the deposition of other forms of energy inside the brain, the targeted delivery of drugs, devices, or cells, will necessitate both a deep understanding of the underlying anatomy and the possibility to acquire detailed images before, during and after the treatment. More generally, the progressive understanding of the brain connectivity is particularly challenging for the description of the human connectome (Bullmore and Sporns, 2009).

Disclosure of interest

No author received financial support in conjunction with the generation of the submission; no author has any personal or institutional financial interest in materials, or devices described in their submissions; Laurent Hermoye and Wojciech Gradkowski are, respectively, the head and an employee of Imagilys; this study does not use or promote Imagilys's products, there is no conflict of interest between Imagilys and this study.

Acknowledgments

This study was supported by the Institute for the Encouragement of Scientific Research and Innovation of Brussels (IRSIB), Government of Brussels-Capital Region, Belgium, the Fond National de la Recherche Scientifique (FNRS), Belgium, and NIH/NIA grant #AG20012. We thank Andrew Frew (PhD, UCLA, USA) for his editorial advice.

We want to pay homage to all the pioneers in neuroanatomy for their extensive and meticulous work that has fostered research in this field and yielded a tremendous amount of pertinent and robust data.

Appendix A. Supplementary data

Supplementary data associated with this article can be found, in the online version, at doi:10.1016/j.neuchi.2011.04.001.

References

Andrade, D.M., et al., 2006. Long-term follow-up of patients with thalamic deep brain stimulation for epilepsy. Neurology 66 (10), 1571–1573.

Aravamuthan, B.R., et al., 2007. Topography of cortical and subcortical connections of the human pedunculopontine and subthalamic nuclei. NeuroImage 37 (3), 694–705.

Basser, P.J., Mattiello, J., LeBihan, D., 1994. MR diffusion tensor spectroscopy and imaging. Biophysical Journal 66 (1), 259–267.

Benabid, A.L., et al., 1996. Chronic electrical stimulation of the ventralis intermedius nucleus of the thalamus as a treatment of movement disorders. Journal of Neurosurgery 84 (2), 203–214.

Bürgel, U., et al., 1999. Mapping of histologically identified long fibre tracts in human cerebral hemispheres to the MRI volume of a reference brain: position and spatial variability of the optic radiation. NeuroImage 10 (5), 489–499.

Bullmore, E., Sporns, O., 2009. Complex brain networks: graph theoretical analysis of structural and functional systems. Nature reviews. Neuroscience 10 (3), 186–198.

Catani, M., Jones, D.K., ffytche, D.H., 2005. Perisylvian language networks of the human brain. Annals of Neurology 57 (1), 8–16.

Dejerine, J., 1901. Anatomie des centres nerveux (Tomes 1 and 2). Rueff et Cie, Paris.

Filley, C., 2001. The behavioural neurology of white matter. Oxford University Press, Oxford.

Forel, A., 1877. Untersuchungen über die haubenregion und ihre oberen verknüpfungen im gehirne des menschen und einiger säugethiere, mit beiträgen

zu den methoden der gehirnuntersuchung. Archiv für Psychiatrie und Nervenkrankheiten 7, 393–495.
Goetz, C.G., 2000. Battle of the titans: Charcot and Brown-Séquard on cerebral localization. Neurology 54 (9), 1840–1847.
Greenberg, B.D., et al., 2006. Three-year outcomes in deep brain stimulation for highly resistant obsessive-compulsive disorder. Neuropsychopharmacology: Official Publication of the American College of Neuropsychopharmacology 31 (11), 2384–2393.
Habas, C., Cabanis, E.A., 2007. Cortical projection to the human red nucleus: complementary results with probabilistic tractography at 3T. Neuroradiology 49 (9), 777–784.
Heimer, L., 2000. Basal forebrain in the context of schizophrenia brain research. Brain Research Reviews 31 (2–3), 205–235.
Hermoye, L., et al., 2006. Pediatric diffusion tensor imaging: normal database and observation of the white matter maturation in early childhood. NeuroImage 29 (2), 493–504.
Herzog, J., et al., 2007. Stimulation of subthalamic fibre tracts reduces dyskinesias in STN-DBS. Movement Disorders: Official Journal of the Movement Disorder Society 22 (5), 679–684.
Hirano, A., Llena, J.F., 1995. Morphology of central nervous system axons. In: Waxman, S.G., Kocsis, J.D., Stys, P.K. (Eds.), The axon: structure, function and pathophysiology. New York Oxford, pp. 49–67.
Jaermann, T., et al., 2004. SENSE-DTI at 3 T. Magnetic Resonance in Medicine: Official Journal of the Society of Magnetic Resonance in Medicine/Society of Magnetic Resonance in Medicine 51 (2), 230–236.
Jiang, H., et al., 2006. DtiStudio: resource program for diffusion tensor computation and fiber bundle tracking. Computer Methods and Programs in Biomedicine 81 (2), 106–116.
Jones, D.K., et al., 2002. Spatial normalization and averaging of diffusion tensor MRI data sets. NeuroImage 17 (2), 592–617.
Laget, P., 1973. Elements de neuro-anatomie fonctionnelle. Masson, Paris.
Lemaire, J., et al., 2007. Brain mapping in stereotactic surgery: a brief overview from the probabilistic targeting to the patient-based anatomic mapping. NeuroImage 37 (Suppl 1), S109–S115.
Leow, A.D., et al., 2009. The tensor distribution function. Magnetic Resonance in Medicine: Official Journal of the Society of Magnetic Resonance in Medicine/Society of Magnetic Resonance in Medicine 61 (1), 205–214.
Morel, A., Magnin, M., Jeanmonod, D., 1997. Multiarchitectonic and stereotactic atlas of the human thalamus. The Journal of Comparative Neurology 387 (4), 588–630.
Mori, S., et al., 1999. Three-dimensional tracking of axonal projections in the brain by magnetic resonance imaging. Annals of Neurology 45 (2), 265–269.
Mori, S., et al., 2005. MRI atlas of human white matter. Elsevier B.V, Amsterdam.
Mori, S., Zhang, J., 2006. Principles of diffusion tensor imaging and its applications to basic neuroscience research. Neuron 51 (5), 527–539.
Mori, S., van Zijl, P.C.M., 2002. Fibre tracking: principles and strategies – a technical review. NMR in Biomedicine 15 (7–8), 468–480.
Nagae-Poetscher, L.M., et al., 2004. High-resolution diffusion tensor imaging of the brain stem at 3 T. American Journal of Neuroradiology 25 (8), 1325–1330.
Nieuwenhuys, R., Voogd, J., Huijzen, C., 1979. The human central nervous system: a synopsis and atlas. Springer-Verlag, Berlin.
Olszewski, J., Baxter, D., 1954. Cytoarchitecture of the brain stem. Karger, Basel.
Oouchi, H., et al., 2007. Diffusion anisotropy measurement of brain white matter is affected by voxel size: underestimation occurs in areas with crossing fibres. American Journal of Neuroradiology 28 (6), 1102–1106.
Peel, T., 1954. The neuroanatomical basis for clinical neurology. McGraw-Hill Book Company, New York.
Petrides, M., Pandya, D.N., 2007. Efferent association pathways from the rostral prefrontal cortex in the macaque monkey. The Journal of Neuroscience: The Official Journal of the Society for Neuroscience 27 (43), 11573–11586.
Riley, H., 1953. An atlas of the basal ganglia brain stem and spinal cord. Williams & Wilkins, Baltimore.
Schaltenbrand, G., Bailey, P., 1959. Introduction to stereotaxis with an atlas of the human brain Georg. Thieme Verlag, Stuttgart.
Schiff, N.D., et al., 2007. Behavioural improvements with thalamic stimulation after severe traumatic brain injury. Nature 448 (7153), 600–603.
Talairach, J., et al., 1957. Atlas d'anatomie stéréotaxique. Repérage radiologique indirect des noyaux gris centraux des régions mésencéphalo-sous-optiques et hypothalamiques de l'homme. Masson et Cie, Paris.
Tuch, D.S., et al., 2003. Diffusion MRI of complex neural architecture. Neuron 40 (5), 885–895.
Yamamoto, T., et al., 2005. Tractography to depict three layers of visual field trajectories to the calcarine gyri. American Journal of Ophthalmology 140 (5), 781–785.